U. S. DEPARTMENT OF THE INTERIOR
U. S. GEOLOGICAL SURVEY

AN EVALUATION OF SEVERAL GEOPHYSICAL METHODS FOR CHARACTERIZING SAND AND GRAVEL DEPOSITS

by

Karl J. Ellefsen[1], Jeffrey E. Lucius[1], and David V. Fitterman[1]

Open-File Report 98–221

---

[1] U. S. Geological Survey, MS 964, Box 25046, Denver, CO 80225–0046

1998

ABSTRACT

A geophysical investigation can provide valuable geologic information needed to characterize sand and gravel deposits and can be an attractive complement to more common characterization methods like drilling. Although such investigations have already been conducted, a comparison of the different geophysical methods used in these investigations apparently has never been done. For this reason, a study was initiated by the Mineral Resources Program of the U. S. Geological Survey. The goal was to determine the advantages and the limitations of different geophysical methods when used to characterize alluvial sand and gravel deposits. The study is focused on those geophysical methods that are commonly available because these are most likely to be used by industry. Furthermore, the study is focused on surface geophysical methods.

Heretofore, four different methods have been evaluated. Three of the four methods — time-domain electromagnetic (TEM) soundings, DC resistivity soundings, and frequency-domain electromagnetic (FEM) profiling — are similar in that they all measure the electrical conductivity of the ground with depth. Ground penetrating radar, however, maps changes in the dielectric permittivity and/or the electrical conductivity with depth. For all four methods, the objective is to relate the measured physical quantity to the stratigraphy of the alluvial sediments.

The comparisons were conducted at two sites in the South Platte River valley, northeast of Denver, Colorado. One site was a transect across the entire South Platte River valley, and the geology here had been determined from 12 test holes. The alluvial sediments consist of gravel, sand, and some clay, and the sediments are covered with soil that is 1 to 2 m thick. In the center of the transect, the sediments and the soil are 9 to 16 m thick; on the western and the eastern sides, they are 15 to 25 m thick. The underlying bedrock is mostly shale. Across the entire transect, the water table is believed to be 2 or 3 m below the ground surface. In the center of the transect, the combined thickness of the sediments and the soil was accurately determined with TEM soundings and DC resistivity soundings. On the western and the eastern sides of the transect, the thickness was not determined with either method because sedimentary layers that are not present in the test holes or the water table were detected. Ground penetrating radar could not detect any sediments beneath the soil because the soil is clay-rich.

The other site was adjacent to an active sand and gravel pit, where the sediments and the bedrock are well exposed. These alluvial sediments are roughly 7 m thick and consist of gravel, sand, and some clay. The bedrock beneath these sediments is mudstone. The water table is within the alluvial sediments — there are roughly 6 m of unsaturated sediments and 1 m of saturated sediments. The thickness of the unsaturated sediments was accurately determined with TEM soundings and DC resistivity soundings; it was determined less accurately with FEM profiling. The thickness of the saturated sediments could not be determined with any of the tested methods because its electrical conductivity is practically identical to that of saturated bedrock. Sedimentary structures, such as foreset beds, were

detected with ground penetrating radar; the bedrock surface was possibly detected when a low frequency, high-power radar antenna was used.

CONTENTS

LIST OF FIGURES

LIST OF TABLES

1. INTRODUCTION

Geologic information about sand and gravel deposits is used by state governments, local governments, and aggregate companies to plan for the mining of these deposits (Langer and Glanzman, 1993). Usually this geologic information is obtained from exposed sediments in existing pits and from drilling. An attractive complement to these frequently-used methods is a geophysical investigation, and indeed such investigations have been used during the past fifty years to characterize sand and gravel deposits (Wilcox, 1944; Jacobson, 1955; Shelton, 1972; Middleton, 1977; Singhroy and Barnett, 1984; Odum and Miller, 1988; Auton, 1992; Saarenketo and Maijala, 1994; Timmons, 1995; Jol et al., 1998).

For these geophysical investigations, several different methods have been used: DC resistivity, seismic refraction, airborne electromagnetics, and ground penetrating radar. Apparently, however, a comparison of these different methods has never been done. For this reason, a study was initiated by the Mineral Resources Program of the U. S. Geological Survey. The goal was to determine the advantages and the limitations of several geophysical methods when used to characterize sand and gravel deposits. The study focused on commonly available, surface methods because they are most likely to be used by industry. The results of this study should help geologists, geophysicists, and mining engineers select an appropriate method for their investigations.

The study was conducted in the South Platte River valley, northeast of Denver, Colorado (Figure 1). One study site was along a transect of the valley (line AA'); the other was adjacent to the Howe Pit where sand and gravel are currently being mined. At both sites, there was detailed information about the sediment thickness and stratigraphy, which were used to evaluate the geophysical results.

2. GEOPHYSICAL METHODS

Although there are a large number of different geophysical methods for characterizing the ground (see, e.g., Telford et al., 1976; Ward, 1990), not all are suitable for characterizing sand and gravel deposits. A suitably chosen method must meet at least three criteria: It must provide useful information, be inexpensive, and quickly provide results. Several different methods meet these criteria, and four were evaluated.

All four methods are affected by a physical property of the ground that is called "electrical resistivity." To understand this, consider a cylindrical sample of rock, having length l and cross-sectional area A. Its resistivity $\rho = RA/l$ where R is the familiar electrical resistance; because of the normalization by A/l, resistivity does not depend upon the size of the sample. The unit of measurement is typically an ohm-meter (Ω-m). For some geophysical methods, the measurements are reported as "electrical conductivity," which is the

reciprocal of the resistivity. The unit of measurement is a siemens/meter (S/m), and frequently it is more convenient to use millisiemens/meter (mS/m).

Typical resistivities of common sediments and sedimentary rocks are listed in Table 1. The table shows that for any particular material the resistivity may have a large range; furthermore, the resistivities of clays are generally lower than the resistivities of either sands or gravels. Although it is not directly shown in this table, resistivity is strongly affected by water saturation because electrical current can readily travel through water-filled pores. For this reason, resistivity generally decreases as the saturation increases. Indeed, many of the lower resistivities in this table may be from partially or completely saturated sediments.

2.1 Time-Domain Electromagnetic Soundings

For time-domain electromagnetic (TEM) soundings, the transient induction properties of electromagnetic fields are used to determine the electrical resistivity-depth function at a site (Kaufman and Keller, 1983; Fitterman and Stewart, 1986). The measurement is made by passing a steady current through a square transmitter loop, for which each side is typically 40 m long. The current is abruptly turned off, inducing a circulating current flow in the ground under the loop. As time passes, this current system diffuses downward and outward, much like a descending smoke ring (Nabighian, 1979). The rate of diffusion is controlled by the resistivity of the ground, with the current passing more quickly through more resistive zones than through less resistive zones. Attenuation of the current is greater in the more resistive zones than in the less resistive zones. A multi-turn receiver coil, usually located at the center of the transmitter loop, responds to the magnetic field produced by the decaying current system in the ground. The voltage induced in the receiver coil, called a transient, is recorded. The transmitter waveform is actually a 50-percent duty cycle square wave, resulting in positive and negative transients. Several ten's or hundred's of transients are recorded and averaged to make a single reading. Several readings are measured and further averaged to improve signal quality. The averaged signal is converted to apparent resistivity; this normalization to apparent resistivity makes the comparison of soundings from different locations easy (Fitterman and Stewart, 1986; Spies and Eggers, 1986).

The apparent resistivity-time curves are used to estimate how the electrical resistivity changes with depth. The mathematical model for the estimation consists of a stack of layers, each of which is homogeneous and isotropic. The electric resistivity and the thickness of each layer are determined with the nonlinear least squares method (Anderson, 1982a, 1982b; Interpex, 1996).

2.2 Frequency-Domain Electromagnetic Profiling

For frequency-domain electromagnetic (FEM) profiling, the induction properties of electromagnetic fields are used to determine the electrical resistivity-depth function at a site (McNeill, 1980). This method employs a transmitter loop, which is energized with a

sinusoidally varying current. The transmitter current produces a time varying magnetic field, which induces current flow in the ground. The induced current is phase-shifted 90° from the transmitter current and is inversely proportional to the ground resistivity. A receiver coil senses the magnetic field produced by the transmitter current and the induced current in the ground. Because of the phase shift between these two signals, they can be separated electronically. The primary magnetic field is defined as the field that would be produced by the transmitter current if the conductive ground were absent, and the secondary magnetic field is defined as the field produced only by current flow in the conductive ground. The quadrature (out of phase) component of the ratio of the secondary to primary magnetic field is proportional to the apparent conductivity of the ground. The apparent conductivity is measured at several different transmitter-receiver loop separations and coil orientations because each probes the ground differently and to different depths. The measurements at the short separations were made with an instrument called an "EM31" (Geonics Limited, 1984); the measurements at the intermediate and long separations with an "EM34" (Geonics Limited, 1987).

The measurements of apparent conductivity are used to estimate how the electrical resistivity changes with depth. The mathematical model for the estimation consists of a stack of layers, each of which is homogeneous and isotropic. The electrical resistivity and the thickness of each layer are estimated by the nonlinear least squares method (Anderson, 1992).

FEM measurements were also made at very short loop separations, 1 m, using an "EM38" (Geonics Limited, 1992). Because the loop separation is so small, the measurement is affected primarily by the sediments that are very close to the instrument. For this reason, the apparent conductivity is treated as the true conductivity of the sediments near the instrument.

2.3 DC Resistivity Soundings

For DC resistivity soundings, magnetostatic fields are used to determine the electrical resistivity-depth function at a site (Telford et al., 1976, p. 632–701; Zohdy, 1974, p. 8–55; Koefoed, 1979). A direct current (DC) is introduced into the ground using two metal electrodes, and the potential difference is measured between two other metal electrodes. The configuration of the electrodes is the Schlumberger spread, for which all four electrodes are in a straight line and are symmetric about its midpoint. Sometimes, instead of a direct current, a low-frequency alternating current with a square waveform is used. The measurements are made after the transients have decayed, and the voltages for both directions are averaged to reduce the noise. The separation between the current electrodes is increased to probe the ground to a greater depth, and for each separation the voltage is measured. Each voltage is converted to an apparent resistivity; this normalization to apparent resistivity makes the comparison of soundings from different locations easy.

The measurements of apparent resistivity are used to estimate how the electrical resistivity changes with depth. The mathematical model for the estimation consists of a stack of

layers, each of which is homogeneous and isotropic. The electrical resistivity and the thickness of each layer are estimated by the nonlinear least squares method (Interprex, 1988).

2.4 Ground Penetrating Radar

For ground penetrating radar (GPR), radar waves are used to map changes in electromagnetic properties of the ground (Daniels, 1989; Davis and Annan, 1989; Annan and Cosway, 1992). A radar wave is radiated from a transmitting antenna into the ground. When the wave encounters a change in an electromagnetic property, some of wave is reflected back towards the ground surface where it is detected by a receiving antenna. The voltage at the receiving antenna is recorded; the recording usually starts when the wave is radiated from the transmitting antenna, and it ends after the reflected waves of interest have arrived at the receiving antenna. This recording is called a radar scan.

A typical GPR survey is performed by slowly pulling both the transmitting and the receiving antennas across the ground surface, usually along a straight line. Along each line, many radar scans are recorded to densely probe the ground. Sometimes a survey is performed with several antennas, each having a different frequency range: Antennas with a high frequency range detect both large and small features at shallow depths only. In contrast, antennas with a low frequency range detect only large features at shallow and moderate depths. The frequency range is usually specified by the "center frequency," which is defined as the frequency component having the highest amplitude when the antenna is suspended in air.

For typical processing, the radar scans are filtered to remove random noise, and they are moved to their correct location along the survey line. The radar scans are displayed together as an image, which looks somewhat like a cross section of the ground.

3. TRANSECT OF THE SOUTH PLATTE RIVER VALLEY

3.1 Geology

The South Platte River valley is filled with alluvial sediments that were eroded from the Rocky Mountains (Colton, 1978; Scott, 1965; Trimble and Machette, 1979; Wayne et al., 1991). Within the portion of the valley that is pertinent to this investigation (Figure 1), there are two landforms: the high terrace and the low terrace. Beneath the high terrace are sediments of late Pleistocene age; beneath the low terrace are sediments of Holocene age. The low terrace includes the modern floodplain.

Both landforms are crossed by transect *AA'* (Figure 1), which parallels Road 28. Alongside this road, the sediments were drilled and logged by the Water Resources Division of the U. S. Geological Survey (Schneider, 1962). From these logs, cross sections were made (Figures 2 and 3). Beneath the eastern high terrace, the sediments are about 15 m thick and consist of sand and gravel. Beneath the western high terrace, the

sediments range from 19 to 25 m thick and consist of clay, sand, and gravel. Beneath the low terrace, the sediments range from 9 to 16 m thick and consist of sand and gravel. Both terraces are covered with soil that is roughly 1 or 2 m thick. The bedrock is the Laramie Formation; in most test holes this bedrock was logged as shale, although in a few it was logged as coal or sandstone.

Schneider (1962, p. 14–16) reports depths to the water table that were measured in wells near the transect. These measurements were made during the 1940's and 1950's, and whether they are similar to the present depths is not known. At that time, the water table was roughly 2 m beneath the eastern high terrace, 2 to 3 m beneath the low terrace, and 10 m beneath the western high terrace.

3.2 Geophysical Results

The purpose of making the geophysical measurements was to determine the thickness of the alluvial sediments and their stratigraphy. To this end, three different geophysical methods were tested: TEM soundings, DC resistivity soundings, and GPR. All measurements were made in fields alongside Road 28. Adjacent to and within these fields were electrical power lines and pipelines from oil and gas wells. Since both could affect the geophysical measurements, the locations for the measurements had to be carefully chosen. As a consequence, the measurements are sparse.

Six TEM soundings were made along transect *AA'* (Figure 2). From these soundings, electrical models of the ground were developed using the procedures described in Section 2.1. The four models that are all within the low terrace are somewhat similar. The first layer has resistivities between 31 and 45 Ω-m; the second layer between 13 and 20 Ω-m. The boundary between the first and the second layers is approximately at the boundary between the sediments and the bedrock. The first layer is interpreted as equivalent to three geologic layers: the soil, the unsaturated alluvial sediments, and the saturated alluvial sediments; the second layer is interpreted as the bedrock. The electrical models at 1400 and 5000 m do not correspond to the proposed geology (Lindsey, D. A., 1998, unpub. data), and with both models the thickness of the alluvial sediments was not determined. The layers in these electrical models may correspond to sedimentary layers that are absent at the test holes, which in both cases are roughly 500 m from the sounding. Alternatively, the layers in these electrical models may correspond to the water table.

Seven DC resistivity soundings were made along transect *AA'* (Figure 3). From these soundings, electrical models of the ground were developed using the procedures described in Section 2.3. In all electrical models, the resistivities of the first layer are low; it is interpreted as the clay-rich soil. In the model at 1900 m, the second layer is interpreted as alluvial sediments, probably sand and gravel; the third layer is interpreted as clay. In the models at 3300 and 3600 m, the second layer is interpreted as alluvial sediments; the third layer is interpreted as bedrock. The models at 4100 and 4200 m are unreliable — here a farmer had scrapped the soil and upper sediments to build a levee along the South Platte River. Likewise, the model at 4800 m is unreliable probably because pipes and electrical

power lines were close to the electrode spread. The model at 5000 m does not correspond to the proposed geology (Lindsey, D. A., 1998, unpub. data), and the thickness of the alluvial sediments was not determined. The layers in this model may correspond to sedimentary layers that are absent at the test hole, which is roughly 500 m from the sounding.

At about 3200 m in transect *AA'* (Figure 2), three sets of GPR data were collected (Figure 4); the data were processed using the methods described in Section 2.4. All three sets lack any feature that may be related to a structure in the soil or the sediments. Rather, all three are somewhat similar: They are dominated by equally-spaced, horizontal, black and white lines. (The spacing depends upon the antenna — the spacing increases as the center frequency of the antenna decreases. These lines change abruptly in the horizontal direction because the electromagnetic coupling between the antenna and the ground changes.) This phenomenon, which is called "antenna ringing," is caused by a material with a low electrical resistivity that is close to the antenna; this material is the clay-rich soil. Because of this antenna ringing, these radar data contain no useful information about the geology.

4. HOWE PIT

4.1 Geology

The sediments at the Howe Pit underlay the low terrace of the South Platte River valley (Figure 1). There are four distinct sedimentary layers (Lindsey et al., 1998):

1. Soil and overbank deposits. This layer is about 1¼ m thick and consists of three sub-layers, which are soil, fine gravel, and clay.
2. Upper gravel unit. This layer consists of gravel, sand, isolated lenses of clayey overbank sediments, and isolated lenses of silty-clay. At some locations, the gravel and the sand form cross beds, which probably were deposited in a point bar. The lenses of overbank sediments contain organic matter including cottonwood logs. The lenses of silty-clay occur only at the bottom of this unit and are up to 1 m thick.
3. Middle gravel unit. This layer consists of gravel, sand, and isolated lenses of silty-clay.
4. Basal gravel unit. This layer consists of gravel and smaller amounts of sand and clay. The gravel is pebble to cobble size.

Although the thickness of each gravel layer varies, their combined thickness is roughly 7 m. Beneath the sediments at the Howe Pit are the mudstones of the Denver Formation.

Near the Howe Pit are a pond and an abandoned pit; both are filled with water, indicating that the water table is close to the ground surface. The bottom of the Howe Pit is roughly 8 m below the ground surface, and to prevent the pit from filling with water, its north and east walls were sealed with clay. The south and west walls, however, were not sealed because they were being excavated. Along these two walls, ground water seeped from the bottom of the basal gravel into the pit. This water collected in a shallow trench within the bedrock, and then it was pumped out of the pit. Because of this procedure, most of the

sediments near the south and west walls were unsaturated. Only the sediments at the bottom of the basal gravel unit were saturated.

4.2 Geophysical Results

The purpose of making the geophysical measurements was to determine the thickness of the gravel units and their heterogeneity. To this end, four different geophysical methods were tested: TEM soundings, DC resistivity soundings, FEM profiling, and GPR. All measurements were made in the southwest corner of the Howe Pit (Figure 5), where the soil and the overbank deposits had been removed to prepare for mining the three gravel units (see Section 4.1).

In addition to the surface geophysical measurements, the electrical resistivities of the sediments, the bedrock, and the ground water were measured directly. The sediments on the cliff face and the bedrock on the pit floor (Figure 5) were measured in situ using the EM38. Samples of ground water were taken from seepage at the bottom of the basal gravel and from a trench along the base of the cliff, and their resistivities were measured with the Orion conductivity meter (model 126 with conductivity cell no. 012210) (Orion Research Inc., 1990). All resistivities are summarized in a box and whiskers plot (Figure 6); there are three important findings:

- The resistivity for the group "saturated sand & gravel and saturated bedrock" is much lower than the resistivities for the two groups of unsaturated sediments.
- The resistivity for "saturated sand & gravel and saturated bedrock" is similar to that for "ground water." The resistivity of the saturated sediments and the saturated bedrock is probably strongly affected by the ground water.
- The resistivity for "unsaturated sand & gravel" is somewhat similar to that for "unsaturated clay, silt, & channel deposits."

These baseline resistivities were used to interpret the surface geophysical measurements.

Four TEM soundings were made, and then electrical models of the ground were developed using the procedures described in Section 2.1. All electrical models, which are displayed in a cross section (Figure 7), have three layers. The top layer has high resistivities, which are similar to measured resistivities of the unsaturated sediments (Figure 6). Likewise, the middle layer has low resistivities, which are similar to measured resistivities of the saturated sediments and saturated bedrock (Figure 6). The thickness of the top layer is slightly less than the combined thickness of the three gravel units. Therefore, the top layer is interpreted as the unsaturated sediments in the three gravel units. The middle layer is interpreted as both the saturated sediments (in the basal gravel) and the saturated bedrock. The interface between the top and middle layers corresponds to the water table, which gets shallower, going from right to left (northeast to southwest). The bottom layer has very low resistivities and is interpreted as a sedimentary layer within the Denver Formation that is not exposed near the Howe Pit.

Seven DC resistivity soundings were made, and then electrical models of the ground were developed using the procedures described in Section 2.3. The electrical models, which are

displayed in a cross section (Figure 8), have either two or three layers. In the models with two layers, the top layer has high resistivities; in the models with three layers, the top and the middle layers have high resistivities. In both cases, these layers are interpreted as the unsaturated sediments in the three gravel units. The resistivities of these layers are much higher than the baseline resistivities of the unsaturated sediments (Figure 6), a point that will be addressed in Section 5. In all models, the bottom layer, which has low resistivities, is interpreted as both the saturated sediments (in the basal gravel unit) and the saturated bedrock. The layer at about 23 m depth that was detected with the TEM soundings (Figure 7) was not detected with the DC resistivity soundings because of the limited length of the Schlumberger spread.

Along *BB'* (Figure 5), FEM profiling was done with the EM31 and the EM34, and the data were processed using the procedures described in Section 2.2. The electrical models, which are displayed in a cross section (Figure 9), have three layers. The top and middle layers have high and moderate resistivites, respectively; both layers are interpreted as the unsaturated sediments from the three gravel units. Again, the resistivities of these two layers are much higher than the baseline resistivities of the unsaturated sediments (Figure 6), a point that will be addressed in Section 5. The bottom layer has low resistivities, which are similar to the measured resistivities of both the saturated sediments (in the basal gravel unit) and the saturated bedrock (Figure 6). Therefore, the bottom layer is interpreted as the saturated sediments and bedrock. In these models, the interface between the middle and bottom layers is 2 or 3 m deeper than the corresponding interfaces for the TEM models and the DC resistivity models (Figure 7 and 8). The cause of this discrepancy is currently unknown.

Within a rectangular area that was 200 m long and 80 m wide (Figure 5), FEM profiling was done with the EM31 only. Processing was unnecessary — the data were simply contoured (Figure 10). The purpose of these measurements was to determine if this procedure could be used to detect signficant heterogeneity such as a clay layer. The areas with low resistivities are near the unmined gravel units covered with the soil and overbank deposits. Thus, the most likely cause for the low resistivities is the clays from the soil and overbank deposits. In the other areas, the resistivities vary only slightly — most are between 91 and 67 Ω-m. Because the distribution of the resistivities of unsaturated sands and gravels is similar to that of unsaturated clays, silts, and channel deposits (Figure 6), a geological inference about the resistivities in Figure 10 cannot be made. In other words, this procedure cannot be used to detect heterogeneity at this site.

Along the edge of the cliff (Figure 5), GPR data were collected with antennas whose center frequencies were 300 and 500 MHz, and the data were processed using the methods described in Section 2.4. Unlike the data collected along the transect of the South Platte River valley (Figure 4), these radar data show sedimentary structures. The 500 MHz data (Figure 11a) show fine-scale structures to 75 ns in time, which corresponds to roughly 4 m depth. In contrast, the 300 MHz data (Figure 11b) show intermediate-scale structures up to 160 ns, which corresponds to roughly 7 m depth. An obvious sedimentary structure is the foreset beds — in both images, they are between 5 and 50 ns (in time) and

between 10 and 40 m (in horizontal distance). In both images, the regions highlighted with the red rectangles correspond to beds that were exposed in the cliff face (Figure 11c), which was only a few meters from where the data were collected. Both radar images also contain many diffractions, which might be caused by cottonwood logs and the ends of sedimentary beds (see Section 4.1). (A diffraction is scattered radar energy emanating from an abrupt discontinuity in the ground. An example is shown in Figure 11a.) In the 300 MHz data especially on the left side, there is a horizontal reflection at about 160 ns. This reflection is probably related to both the water table and the bedrock surface. These two interfaces are close together — the saturated sediments are probably less than ½ m thick near the cliff edge. This distance is similar to the wavelengths of the radar waves, which are estimated to be between ½ and 1½ m. For this reason, the reflection is probably associated with both interfaces.

5. DISCUSSION

It might be expected that the models derived from the different methods — TEM soundings, the DC resistivity soundings, and the FEM profiling — should be very similar. Indeed, the models for the Howe Pit (Figures 7, 8, and 9) have several similarities:

- For all three methods, the resistivity of the layer (or layers) representing the unsaturated sediments is much higher than the resistivity of the layer representing the saturated sediments and saturated bedrock.
- For all three methods, the resistivities for the layer representing the saturated sediments and saturated bedrock are similar.
- For the TEM and the DC resistivity soundings, the layer representing the saturated sediments and the saturated bedrock is between 7 and 8½ m deep.

Nonetheless, the models from the different methods have some differences:

- The deepest layer in the TEM models is not present in the DC resistivity and FEM models. The most likely cause is that the TEM soundings were able to probe deeper than either the DC resistivity soundings and the FEM profiling.
- The unsaturated sediments are represented by one layer for the TEM soundings, by either one or two layers for the DC resistivity soundings, and by two layers for the FEM profiling. The most likely cause is that the three methods were affected differently by small-scale heterogeneity near the ground surface. For the TEM soundings, this heterogeneity was averaged into the measurements. For the DC resistivity soundings, this heterogeneity was detected only if it was near the center of the Schlumberger spread. Otherwise, it was averaged into the measurements. For the FEM profiling, this heterogeneity was detected by the EM31 measurement.
- For all three methods, the resistivities for the layer (or layers) representing the unsaturated sediments differ greatly. The most likely cause is that the electrical resistivity of the unsaturated sediments is anisotropic. For the TEM soundings, the electrical current travels only in a horizontal direction. For the DC resistivity soundings and the FEM profiling, however, the electrical current travels in both the horizontal and the vertical directions. The resistivities for the horizontal and the vertical directions may differ if, for example, the sediment grains are preferentially aligned. (For the saturated sediments and the saturated bedrock, anisotropy does not

appear to be significant probably because much of the electrical current passes through the water-filled pores.)

Thus, the electrical models from the three methods differ somewhat because each method measured the electrical properties of the ground differently. Nonetheless, the models from all three methods correspond to the geology, indicating that all three methods are suitable for characterizing sand and gravel deposits.

6. CONCLUSIONS

Along the transect of the South Platte River valley, the thickness of the alluvial sediments beneath the low terrace was determined accurately by both TEM and DC resistivity soundings. The thickness beneath the western and the eastern terraces was not determined with either type of sounding; either sedimentary layers that are not present in the test holes or the water table were detected. Ground penetrating radar was unable to map any structures in the alluvial sediments because of the clay-rich soil.

Adjacent to the Howe Pit, the thickness of the unsaturated alluvial sediments was determined accurately with both TEM and DC resistivity soundings; the thickness was determined less accurately with FEM profiling. The thickness of the saturated sediments could not be determined with any of the three methods because its conductivity was practically identical to that of the saturated bedrock. Within a rectangular area 200 m long and 80 m wide, apparent resistivities, which were measured with an EM31, were similar to in situ measurements of unsaturated sand and gravel and of unsaturated clay, silt, and channel deposits. Therefore, these resistivities cannot be used to make a well-substantiated claim about the presence of geologic heterogeneity. Ground penetrating radar detected many structures within the alluvial sediments, especially foreset beds. The bedrock surface and water table together were probably detected when the 300 MHz antennas were used.

This study focused on four different geophysical methods that are commonly available: TEM soundings, DC resistivitiy soundings, FEM profiling, and ground penetrating radar. In most cases, useful geologic information such as sediment thickness could be obtained with these methods; in a few cases, however, the desired information could not be obtained because of the geologic or the hydrologic conditions. We hope that the examples presented in this study will help geologists, geophysicists, and mining engineers select an appropriate method for their geophysical investigations.

7. ACKNOWLEDGMENTS

This work was part of a larger project "Minerals Information and Technology for Infrastructure Resource Assessment," which is funded by the Mineral Resources Program in the U. S. Geological Survey. Jackie Williams, Andrew Hein, and William Langer helped collect data. We are grateful to The Western Mobile Corporation for allowing us to work at the Howe Pit.

8. REFERENCES

Anderson, W.L., 1982a, Adaptive nonlinear least-squares solution for constrained or unconstrained minimization problems, (Subprogram NLSOL): U.S. Geological Survey Open-File Report 82-68, 65 p.

Anderson, W.L., 1982b, Nonlinear least-squares inversion of transient soundings for a central induction loop system (Subprogram NLSTCI): U.S. Geological Survey Open-File Report 82-1129, 85 p.

Anderson, W.L., 1992, Interactive inversion of dipole loop-loop electromagnetic data for layered earth models using numerical integration and complex image theory (Version 1.0): U.S. Geological Survey Open-File Reports 92–553–A and 92–553–B, 42 p.

Annan, A.P., and Cosway, S.W., 1992, Ground penetrating radar survey design: Proceedings of the Symposium on the Application of Geophysics to Engineering and Environmental Problems, April 1992, Oakbrook, Illinois, Society of Engineering and Mineral Exploration Geophysicists, p. 329–351.

Auton, C. A., 1992, The utility of conductivity surveying and resistivity sounding in evaluating sand and gravel deposits and mapping drift sequences in northeast Scotland: Engineering Geology, v. 32, p. 11–28.

Colton, R.B., 1978, Geologic map of the Boulder-Fort Collins-Greeley area, Front Range Urban Corridor, Colorado: U. S. Geological Survey Miscellaneous Investigations Map I-855-F, scale 1:100,000.

Daniels, J.J., 1989, Fundamentals of ground penetrating radar survey design: Proceedings of the Symposium on the Application of Geophysics to Engineering and Environmental Problems, March 1989, Golden, Colorado, Society of Engineering and Mineral Exploration Geophysicists, p. 62–142.

Davis, J.L., and Annan, A.P., 1989, Ground penetrating radar for high resolution mapping of soil and rock stratigraphy: Geophysical Prospecting, v. 37, p. 531–551.

Fitterman, D.V., and Stewart, M.T., 1986, Transient electromagnetic sounding for groundwater: Geophysics, v. 51, p. 995–1005.

Geonics Limited, 1984, Operating manual for EM31-D non-contacting terrain conductivity meter: Geonics Limited, 1745 Meyerside Dr., Unit 8, Mississauga, Ontario, Canada, L5T1C5.

Geonics Limited, 1987, EM34-3 operating instructions: Geonics Limited, 1745 Meyerside Dr., Unit 8, Mississauga, Ontario, Canada, L5T1C5.

Geonics Limited, 1992, EM38 operating manual: Geonics Limited, 1745 Meyerside Dr., Unit 8, Mississauga, Ontario, Canada, L5T1C5.

Interpex, 1988, RESIX-IP User's Manual: Interpex Limited, Golden, Colorado.

Interpex, 1996, TEMIX XL User's Manual (2 vol.): Interpex Limited, Golden, Colorado.

Jacobson, R.P., 1955, Geophysical case history of a commercial gravel deposit: Mining Engineering, v. 7, p. 158–162.

Jol, H.M., Parry, D., Smith, D.G., 1998, Ground penetrating radar: Applications in sand and gravel exploration *in* Bobrowsky, P. T., 1998, Aggregate resources: A global perspective: Rotterdam, A. A. Balkema, Inc., p. 295–306.

Kaufman, A.A., and Keller, G.A., 1983, Frequency and transient sounding: Amsterdam, Elsevier, 685 p.

Koefoed, O., 1979, Geosounding principles: 1. Resistivity sounding measurements: New York, Elsevier Scientific Pub. Co., 276 p.

Langer, W.H., and Glanzman, V.M., 1993, Natural aggregate: Building America's future: U. S. Geological Survey Circular 1110, 39 p.

Lindsey, D.A., and Shary, J.F., 1997, Field measures of gravel quality in the South Platte River north of Denver, Colorado: A pilot study: U. S. Geological Survey Open-File Report 97-451, 19 p.

Lindsey, D.A., Langer, W.H., Cummings, L. Scott, and Shary, J.F., 1998, Gravel deposits of the South Platte River valley north of Denver, Colorado, Part A: Stratigraphy and sedimentary structures: U. S. Geological Survey Open-File Report 98–148–A, 18 p.

McNeill, J.D., 1980, Electromagnetic terrain conductiivty measurement at low induction numbers: Technical Note TN-6, Geonics Limited, Mississauga, Ontario, Canada, 15 p.

Middleton, R.S., 1977, Ground and airborne geophysical studies of sand and gravel in the Toronto region, Ontario Geological Survey Study GS18, 37 p.

Nabighian, M.N., 1979, Quasi-static transient response of a conducting half-space — an approximate representation: Geophysics, v. 44, p. 1700–1705.

Odum, J.K., and Miller, C.H., 1988, Geomorphic, seismic, and geotechnical evaluation of sand and gravel deposits in the Sheridan, Wyoming, area: U. S. Geological Survey Bulletin 1845, 32 p.

Orion Research Inc., 1990, Model 126 and 127 conductivity meter instruction manual: Orion Research Inc., Laboratory Products Group, The Schrafft Center, 529 Main St., Boston, MA 02129.

Parasnis, D.S., 1979, Principles of applied geophysics: London, Chapman and Hall Ltd., 275 p.

Palacky, G.J., 1988, Resistivity characteristics of geologic targets *in* Nabighian, M. N., Electromagnetic methods in applied geophysics — Theory, Vol. I: Tulsa, Oklahoma, Society of Exploration Geophysicists, p. 53–129.

Saarenketo, T., and Maijala, P., 1994, Applications of geophysical methods to sand, gravel and hard rock aggregate prospecting in Northern Finland *in* Lüttig, G. W., 1994, Aggregates — Raw Materials Giant. Report on the 2nd International Aggregates Symposium, Erlangen, Germany, October 22–27, 1990, p. 109–123.

Schneider, P.A. Jr., 1962, Records and logs of selected wells and test holes, and chemical analyses of ground water in the South Platte River basin in western Adams and southwestern Weld Counties, Colorado: Colorado Water Conservation Board Basic-Data Report No. 9, 84 p.

Scott, G.R., 1965, Nonglacial Quaternary geology of the southern and middle Rocky Mountains in Wright, H. E., Jr., Frey, D. G., *eds.*, The Quaternary of the United States: Princeton, N. J., Princeton University Press., p. 342–354.

Shelton, D.C., 1972, Thickness of alluvium and evaluation of aggregate resources in the lower Cache La Poudre river valley, Colorado, by electrical resistivity methods: Boulder, Colorado, University of Colorado, M. S. thesis, 67 p.

Singhroy, V. H., and Barnett, P. J., 1984, Locating subsurface mineral aggregate deposits from airborne infrared imagery (reflected and thermal): A case study in southern Ontario: Proceedings of the International Symposium on Remote Sensing of Environment, 3rd Thematic Conference: Remote Sensing for Exploration Geology, p. 523–539.

Spies, B.R., and Eggers, D.E., 1986, The use and misuse of apparent resistivity in electromagnetic methods: Geophysics, v. 51, p. 1462–1471.

Telford, W.M., Geldart, L.P., Sheriff, R.E., and Keys, D.A., 1976, Applied geophysics: New York, Cambridge University Press, 860 p.

Timmons, B. J., 1995, Prospecting for natural aggregates: An update: Rock Products, v. 98, p. 31–37.

Trimble, D.E., and Machette, M.N., 1979, Geologic map of the greater Denver area, Front Range Urban Corridor, Colorado: U. S. Geological Survey Miscellaneous Investigations Map I-856-H, scale 1:100,000.

Ward, S.H., *ed.*, 1990, Geotechnical and environmental geophysics, vols. I, II, and III: Tulsa, Oklahoma, Society of Exploration Geophysicists.

Wayne, W.J. Aber, J.S., Agard, S.S., Bergantino, R.N., Bluemle, J. ., Coates, D. ., Cooley, M. ., Madole, R. ., Martin, J. ., Mears, B., Jr., Morrison, R.B., and Sutherland, W.M., 1991, Quaternary geology of the northern Great Plains *in* Morrison, R.B., *ed.*, Quaternary nonglacial geology: conterminous U. S.: Boulder, Geological Society of America, The Geology of North America, v. K-12, p. 441–476.

Wilcox, S.W., 1944, Sand and gravel prospecting by the earth resistivity method: Geophysics, v. 9, p. 36–46.

Zohdy, A.A.R., 1974, Electrical methods *in* Zohdy, A.A.R., Eaton, G.P., and Mabey, D.R., Application of surface geophysics to ground-water investigations: Techniques of water resources investigations of the U. S. Geological Survey, Book 2, Chapter D1, p. 5–66.

Table 1. Typical resistivities for various geologic materials (Parasnis, 1979, p. 129; Palacky, 1988, p. 100; Telford et al., 1976, p. 455).

Material	Typical Resistivities (Ω-m)
Shales	20-2000
Argillites	10-800
Sandstones	30-4000
Gravels	500-900
Sands	10-800
Clays	1-100

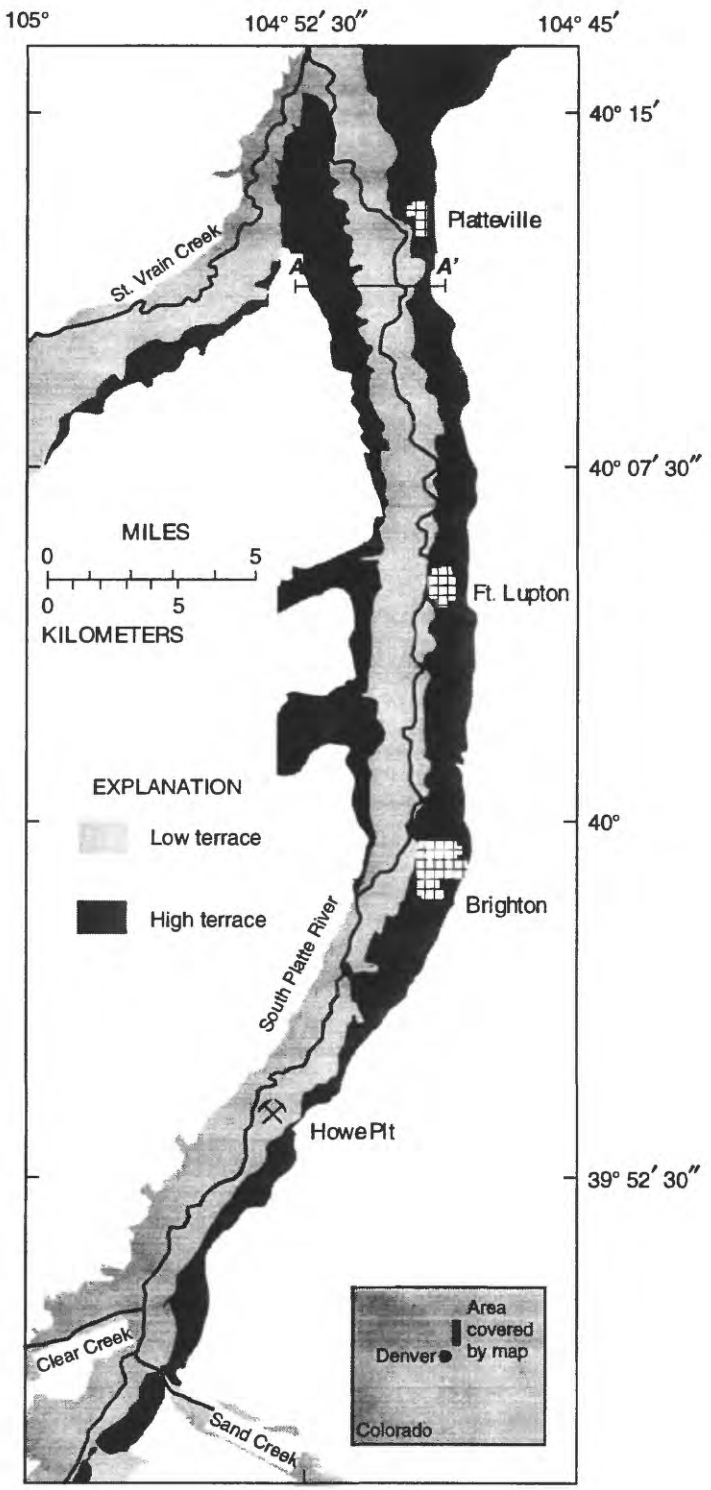

Figure 1. Map of the South Platte River valley where the geophysical studies were conducted (after Lindsey and Shary, 1997). The inset shows the location of the map within Colorado.

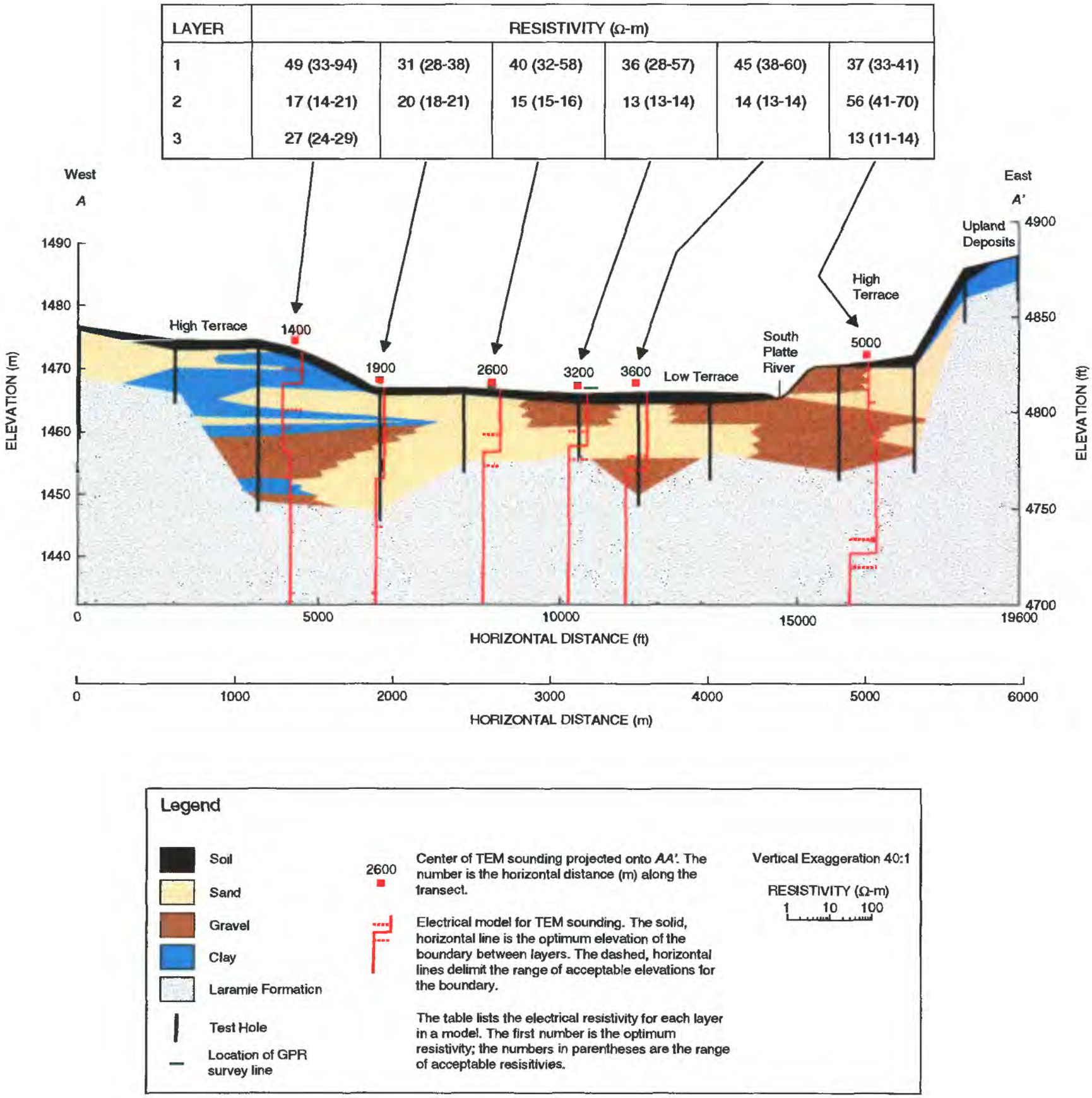

Figure 2. Cross section the South Platte River valley (Lindsey, D. A., 1998, unpub. data) and the electrical models from the TEM soundings. The cross section is along line *AA'* of Figure 1.

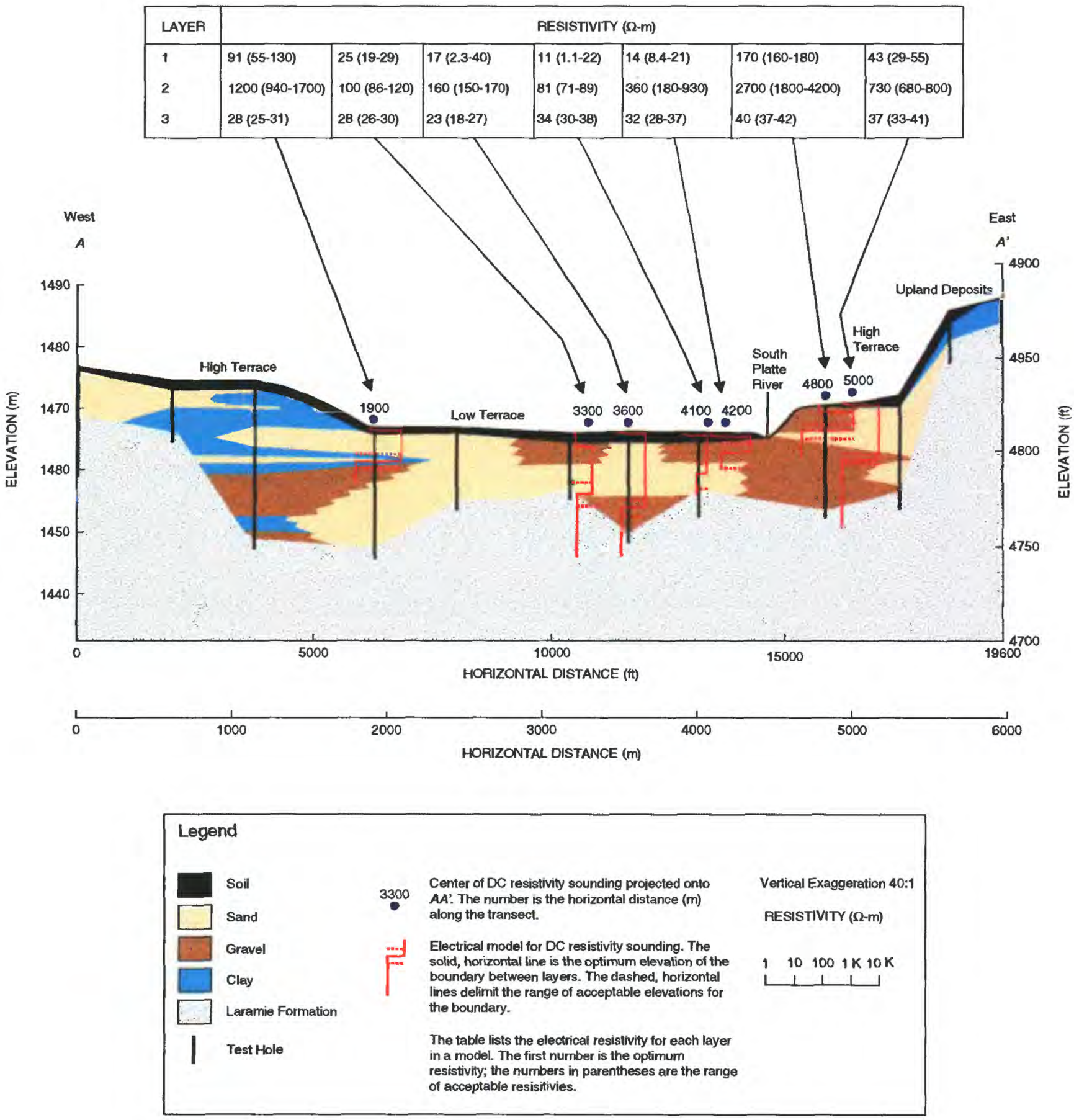

Figure 3. Cross section the South Platte River valley (Lindsey, D. A., 1998, unpub. data) and the electrical models from the DC resistivity soundings. The cross section is along line *AA'* of Figure 1.

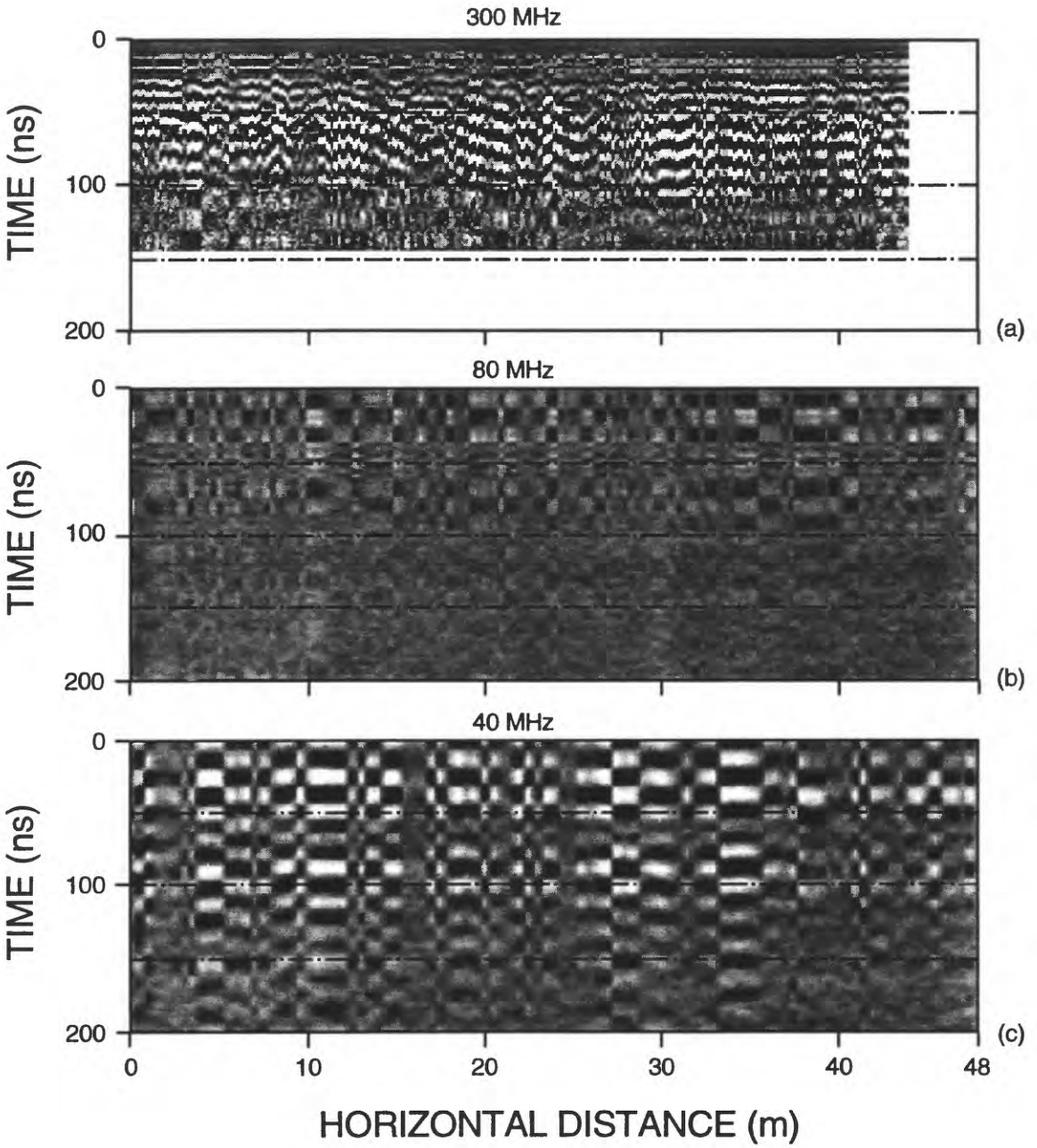

Figure 4. GPR data for center frequencies of (a) 300 MHz, (b) 80 MHz, and (c) 40 MHz. The data were collected at 3200 m (horizontal distance) along the transect of the South Platte River valley (Figure 2).

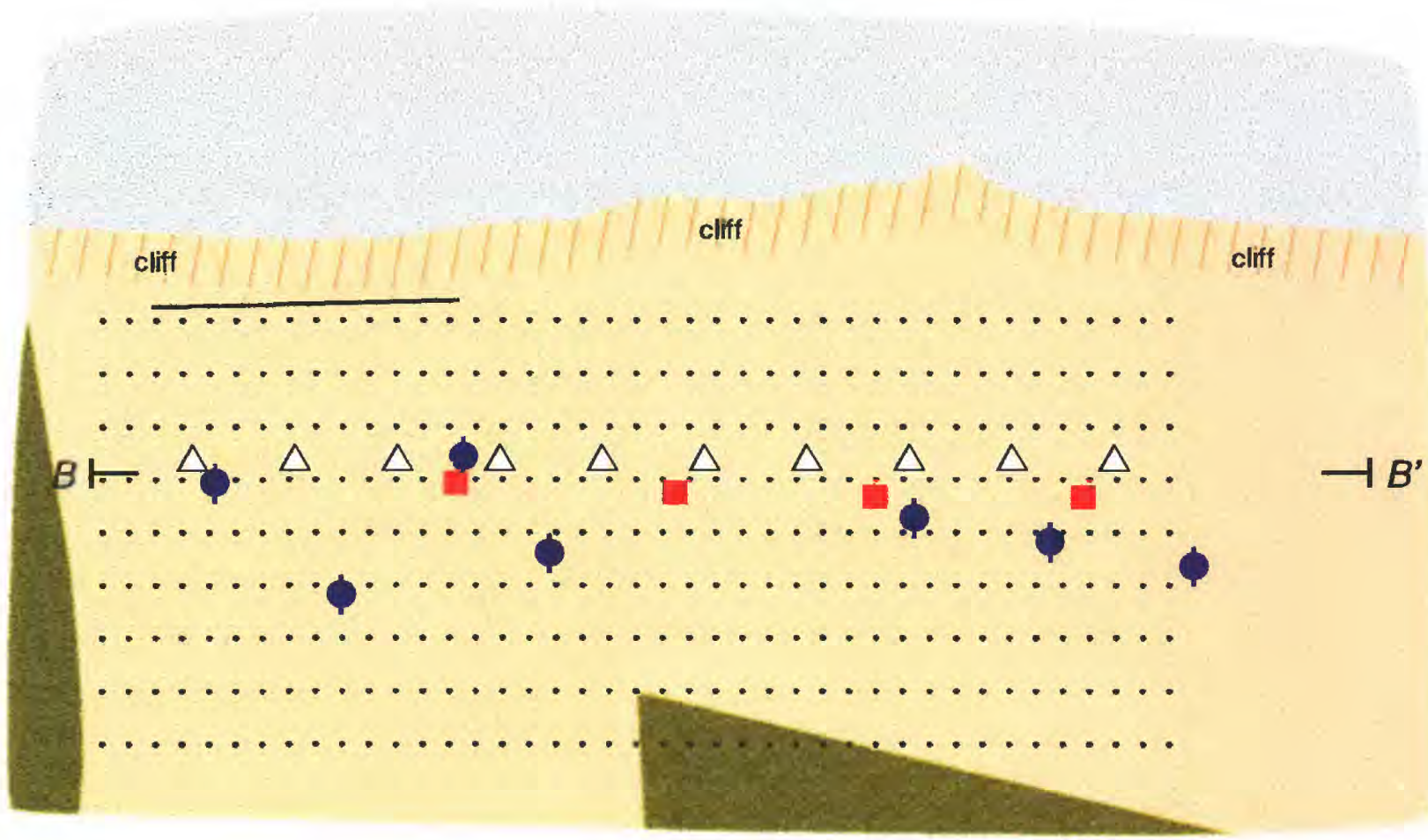

Figure 5. Map of the southwest corner of the Howe Pit showing where the geophysical measurements were made.

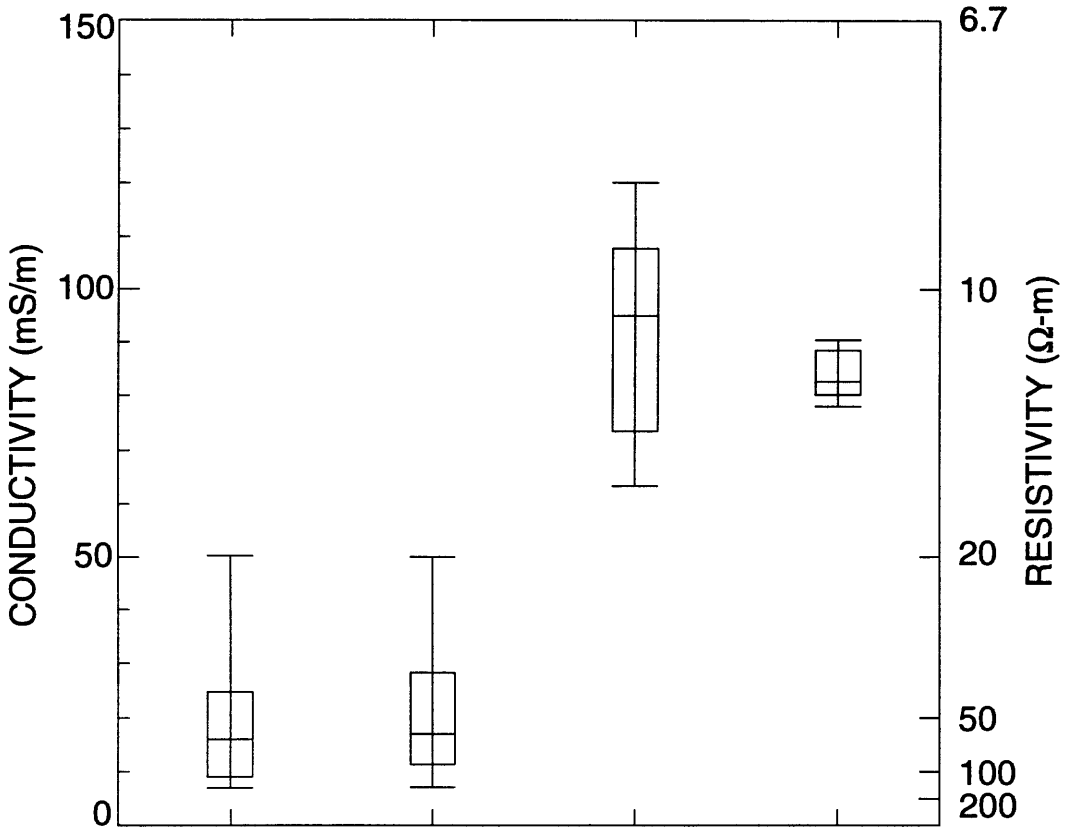

Material	unsaturated sand & gravel (upper, middle and basal gravel units)	unsaturated clay, silt, & channel deposits (upper and middle gravel units)	saturated sand & gravel (basal gravel unit) & saturated bedrock	ground water
Location of Measurements	cliff face	cliff face	cliff face and pit	base of cliff and trenches within pit
Number of Measurements	36	25	7	8
Instrument used for Measurement	EM38	EM38	EM38	Orion Conductivity Meter

Figure 6. Electrical resistivities of various materials at the Howe Pit. The distribution for each material is shown as a box and whisker.

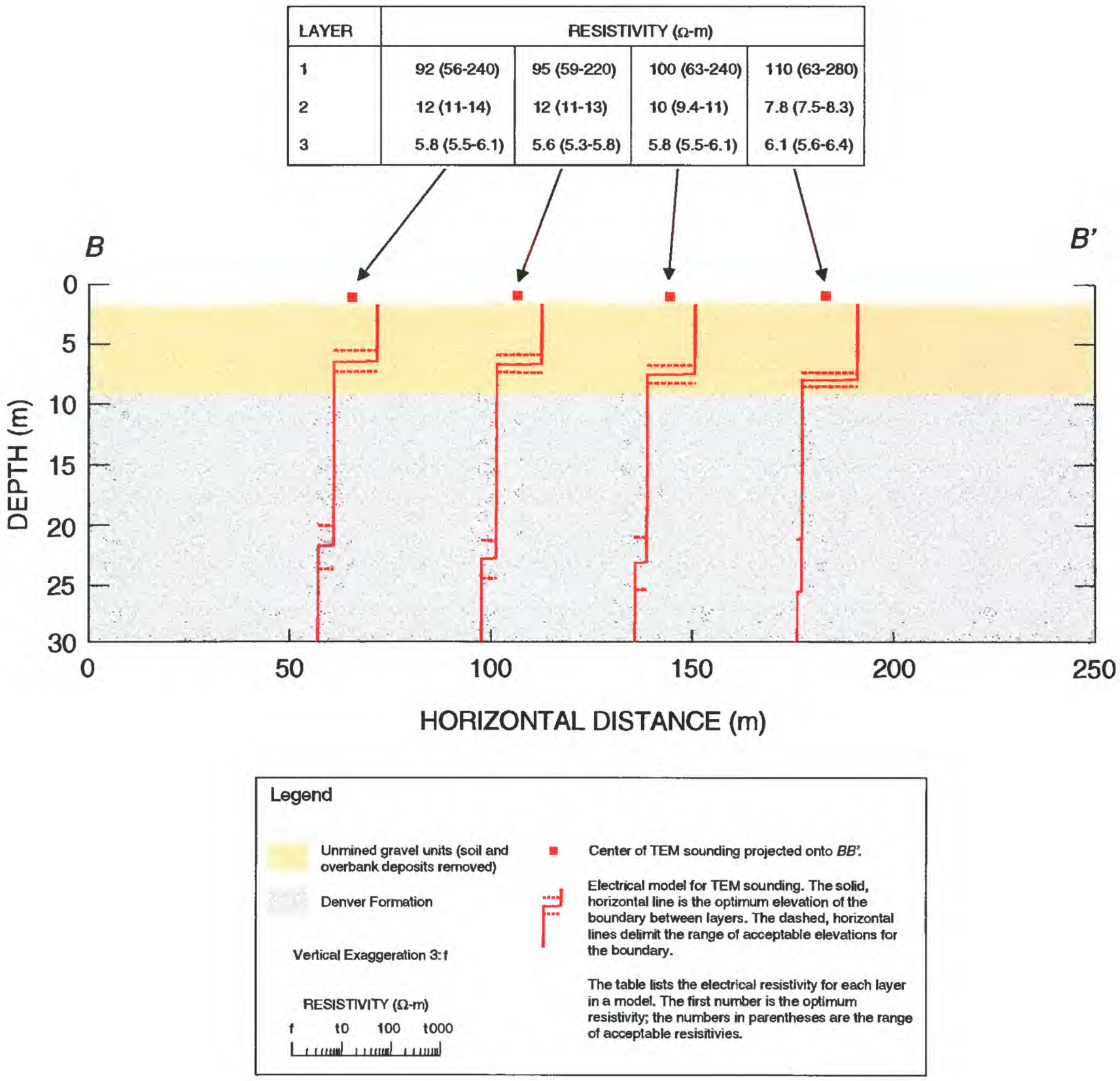

Figure 7. Cross section the Howe Pit (along line *BB'* of Figure 5) and the electrical models from the TEM soundings. The depth to the Denver Formation was measured at the base of the cliff and then projected into this cross section.

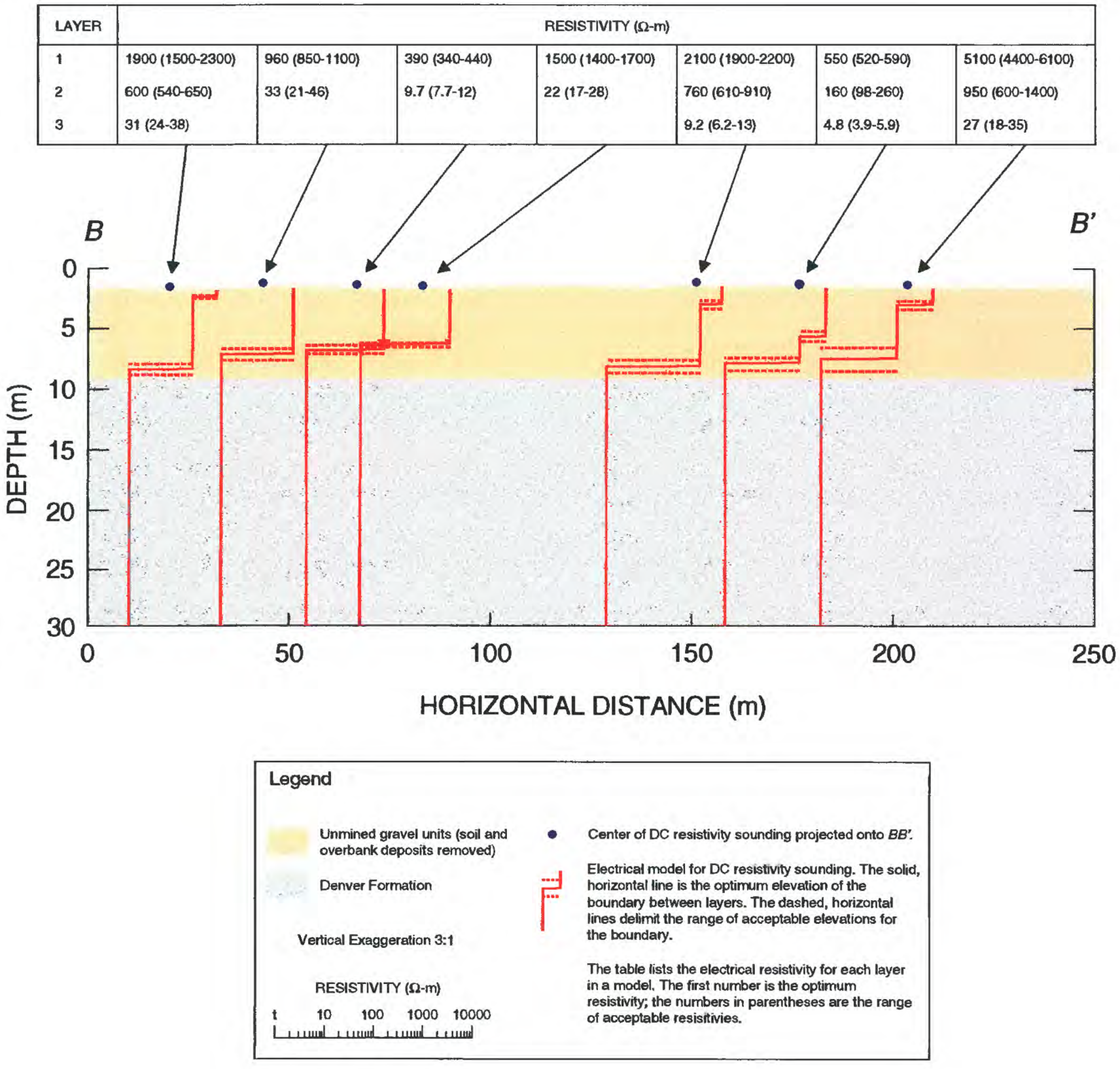

Figure 8. Cross section the Howe Pit (along line *BB'* of Figure 5) and the electrical models from the DC resistivity soundings. The depth to the Denver Formation was measured at the base of the cliff and then projected into this cross section.

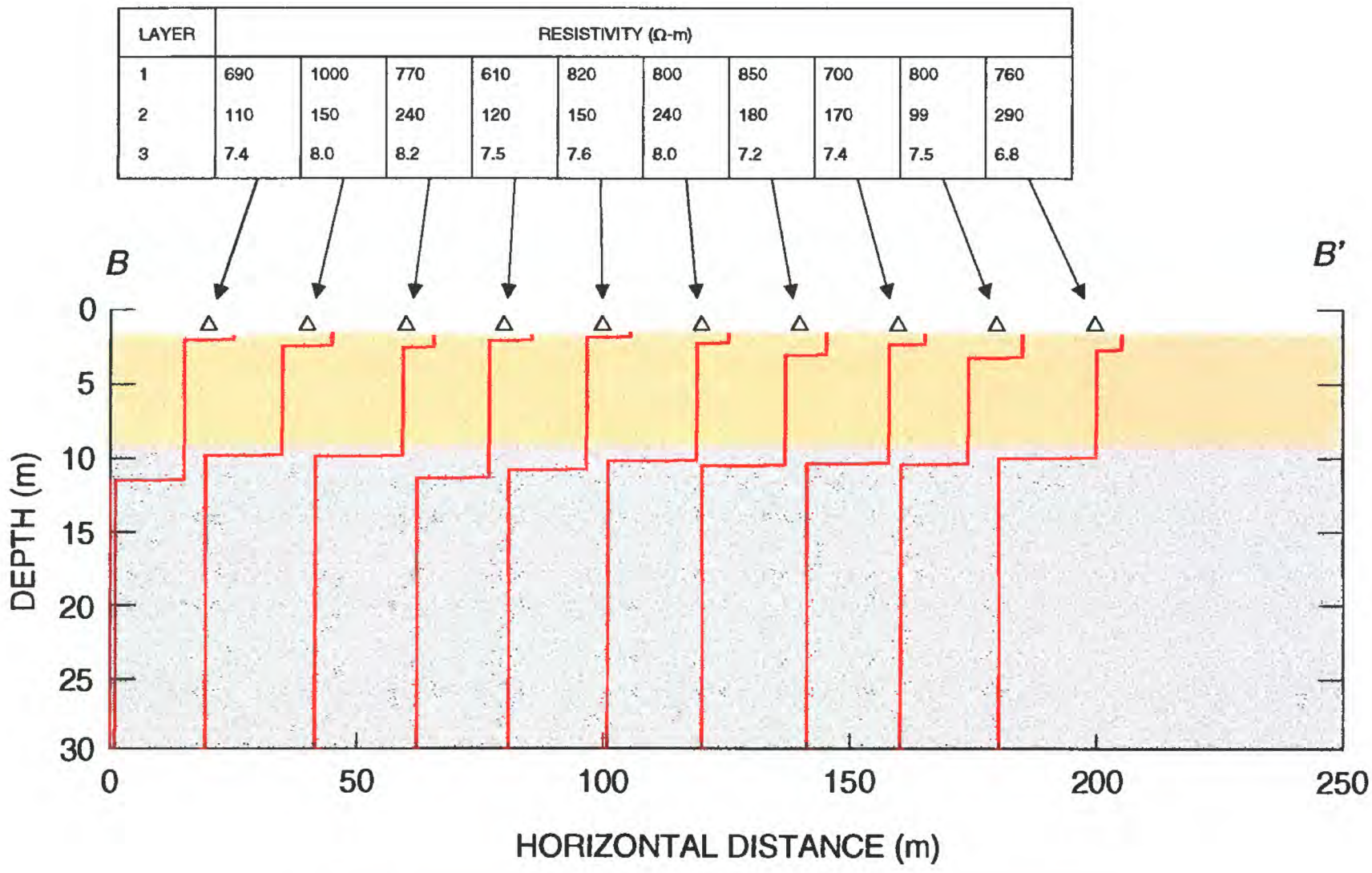

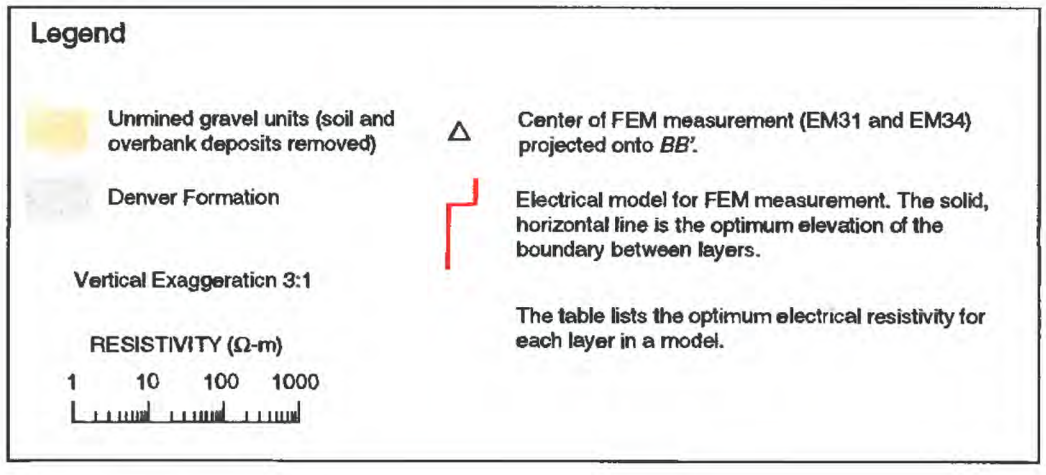

Figure 9. Cross section the Howe Pit (along line *BB'* of Figure 5) and the electrical models from the FEM profiling. The depth to the Denver Formation was measured at the base of the cliff and then projected into this cross section.

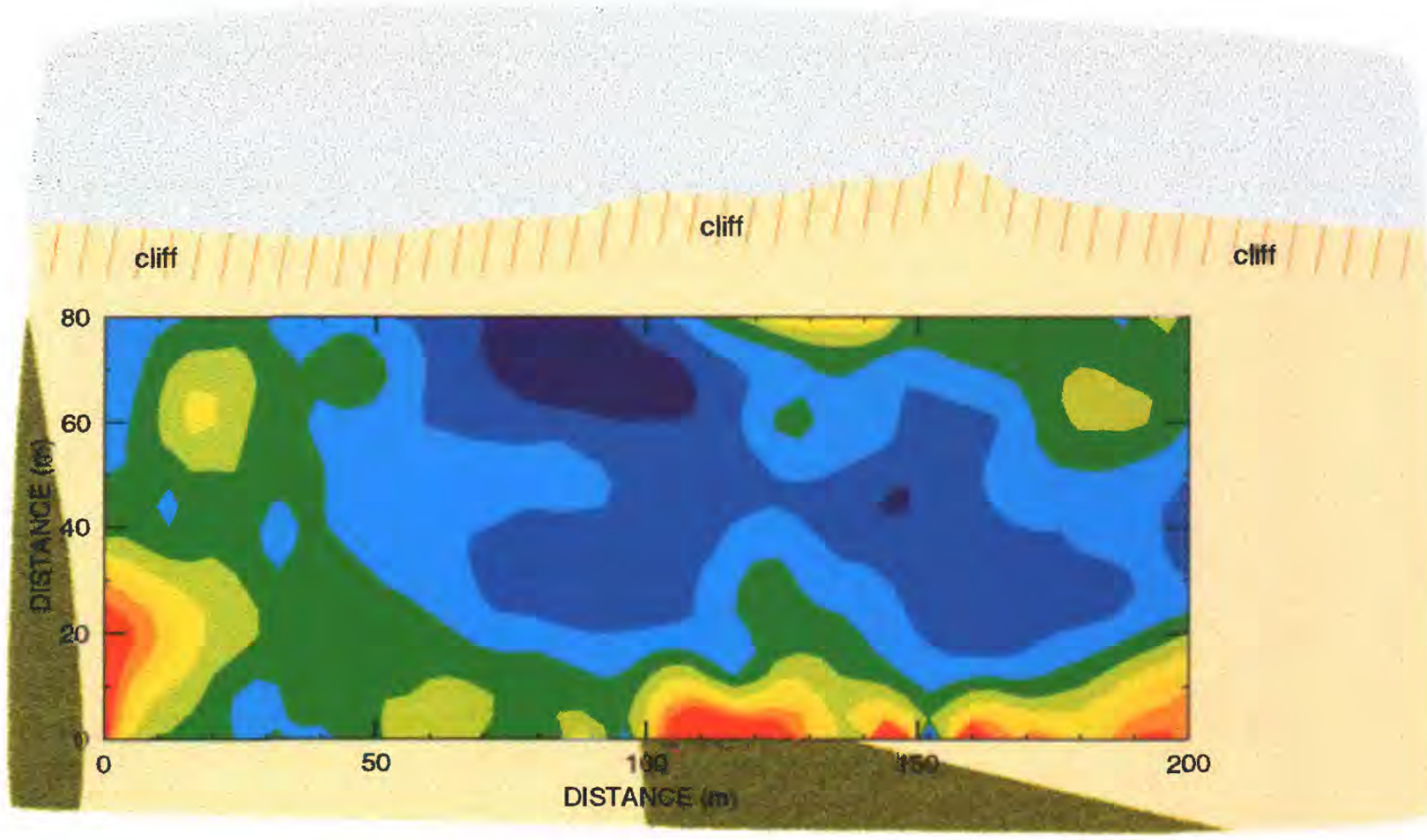

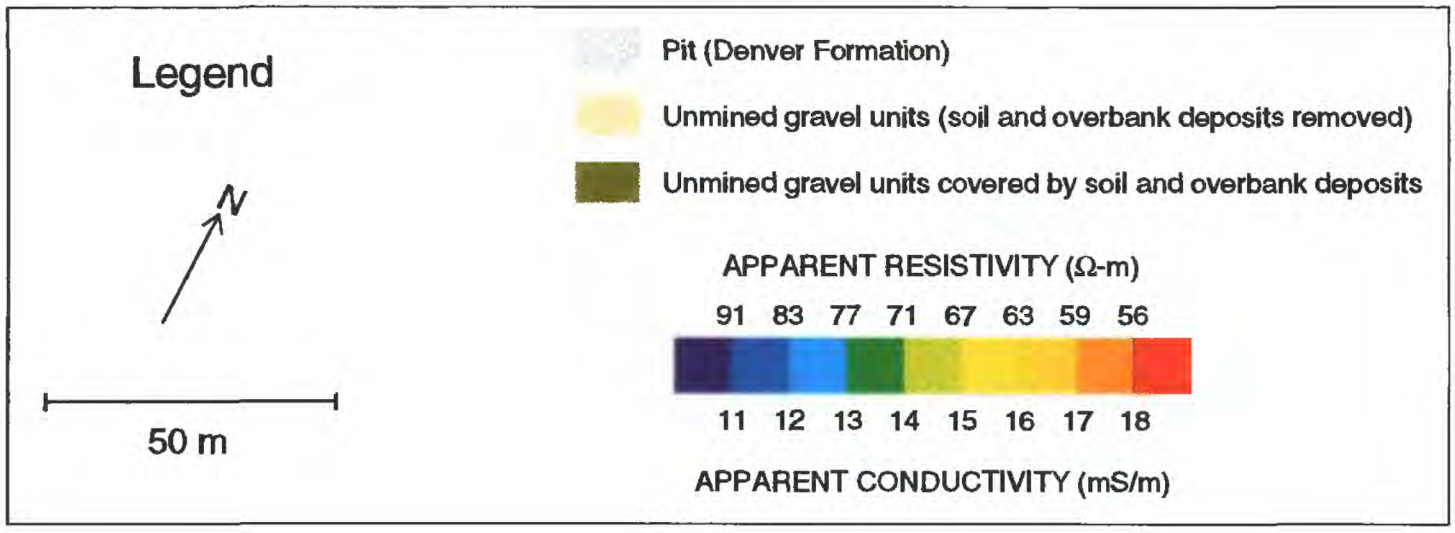

Figure 10. Apparent resistivity measured with the EM31. The location of each measurement is shown in Figure 5.

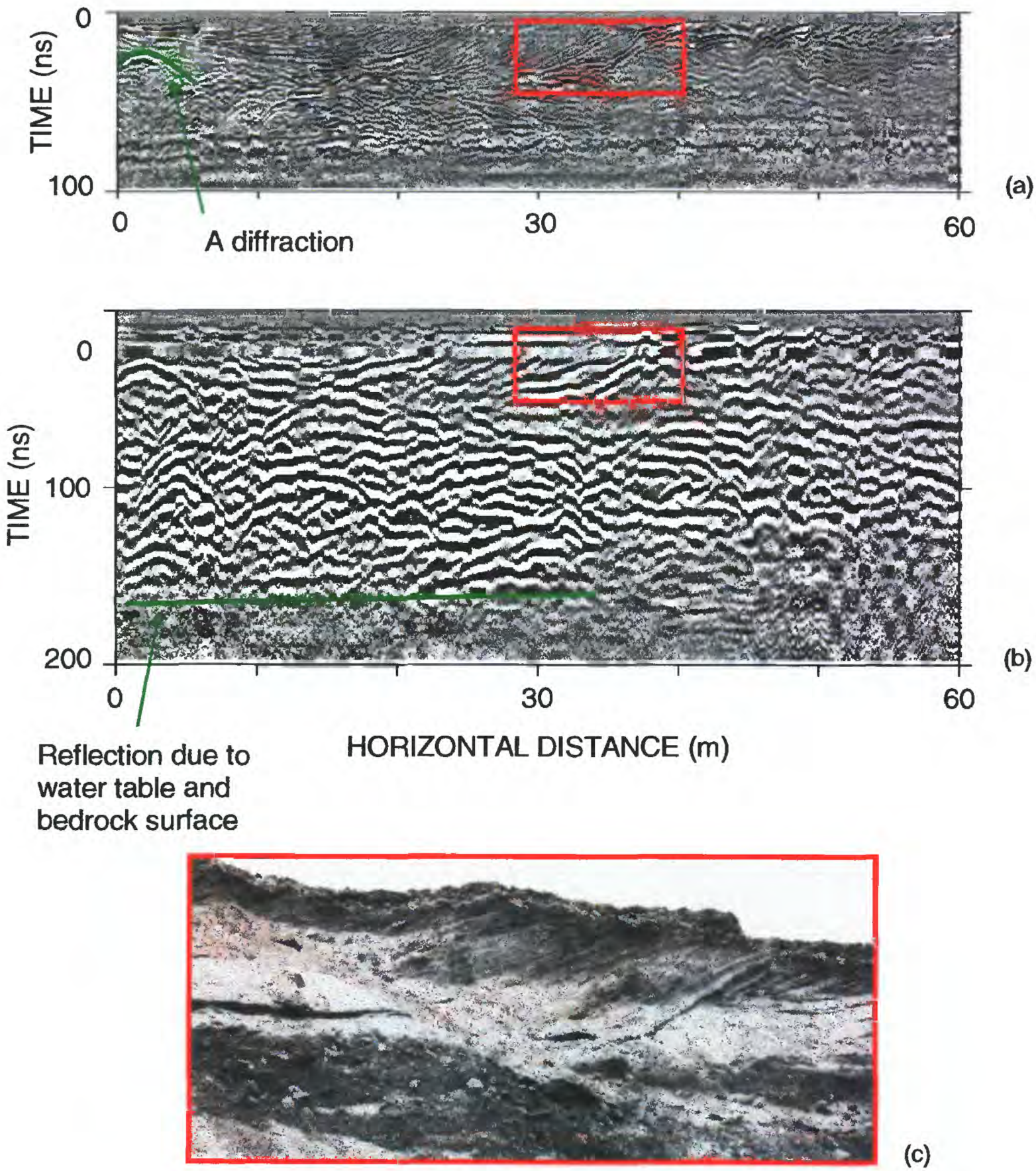

Figure 11. GPR data for center frequencies of (a) 500 MHz and (b) 300 MHz. The location of the GPR survey line is shown in Figure 5; the data are plotted from northeast to southwest, the perspective that an observer inside the pit would have. (c) Picture of foreset beds, which are in the upper gravel unit and are exposed by the cliff. The picture corresponds to the regions in (a) and (b) outlined by red rectangles.